Journal of Physics G: Nuclear and Particle Physics

Exclusive J/ψ and $\psi(2S)$ production in pp collisions at $\sqrt{s} = 7$ TeV

To cite this article: R Aaij *et al* 2013 *J. Phys. G: Nucl. Part. Phys.* **40** 045001

OPEN ACCESS
IOP PUBLISHING JOURNAL OF PHYSICS G: NUCLEAR AND PARTICLE PHYSICS

J. Phys. G: Nucl. Part. Phys. **40** (2013) 045001 (17pp) doi:10.1088/0954-3899/40/4/045001

Exclusive J/ψ and $\psi(2S)$ production in pp collisions at $\sqrt{s} = 7$ TeV

R Aaij[1], C Abellan Beteta[2,3], A Adametz[4], B Adeva[5], M Adinolfi[6], C Adrover[7], A Affolder[8], Z Ajaltouni[9], J Albrecht[10], F Alessio[11], M Alexander[12], S Ali[1], G Alkhazov[13], P Alvarez Cartelle[5], A A Alves Jr[11,14], S Amato[15], Y Amhis[16], L Anderlini[17,18], J Anderson[19], R Andreassen[20,25], R B Appleby[21], O Aquines Gutierrez[22], F Archilli[23], A Artamonov[24], M Artuso[25], E Aslanides[7], G Auriemma[14,26], S Bachmann[4], J J Back[27], C Baesso[28], V Balagura[29,15], W Baldini[30], R J Barlow[21], C Barschel[11], S Barsuk[16], W Barter[31], T Bauer[1], A Bay[32], J Beddow[12], I Bediaga[33], S Belogurov[29,15], K Belous[24], I Belyaev[29,15], E Ben-Haim[34], M Benayoun[34], G Bencivenni[23], S Benson[35], J Benton[6], A Berezhnoy[36], R Bernet[19], M-O Bettler[31], M van Beuzekom[1], A Bien[4], S Bifani[37], T Bird[21], A Bizzeti[17,38], P M Bjørnstad[21], T Blake[11], F Blanc[32], C Blanks[39], J Blouw[4], S Blusk[25], A Bobrov[40,41], V Bocci[14], A Bondar[40,41], N Bondar[13], W Bonivento[42], S Borghi[21], A Borgia[25], T J V Bowcock[8], E Bowen[19], C Bozzi[30], T Brambach[10], J van den Brand[43,44], J Bressieux[32], D Brett[21], M Britsch[22], T Britton[25], N H Brook[6], H Brown[8], I Burducea[45], A Bursche[19], J Buytaert[11], S Cadeddu[42], O Callot[16], M Calvi[46,47], M Calvo Gomez[2,3], A Camboni[2], P Campana[11,23], A Carbone[48,49], G Carboni[50,51], R Cardinale[52,53], A Cardini[42], H Carranza-Mejia[35], L Carson[39], K Carvalho Akiba[15], G Casse[8], M Cattaneo[11], C Cauet[10], M Charles[54], P Charpentier[11], P Chen[32,55], N Chiapolini[19], M Chrzaszcz[56], K Ciba[11], X Cid Vidal[5], G Ciezarek[39], P E L Clarke[35], M Clemencic[11], H V Cliff[31], J Closier[11], C Coca[45], V Coco[1], J Cogan[7], E Cogneras[9], P Collins[11], A Comerma-Montells[2], A Contu[42], A Cook[6], M Coombes[6], G Corti[11], B Couturier[11], G A Cowan[32], D Craik[27], S Cunliffe[39], R Currie[35], C D'Ambrosio[11], P David[34], P N Y David[1], I De Bonis[57], K De Bruyn[1], S De Capua[21], M De Cian[19], J M De Miranda[33], L De Paula[15], W De Silva[20,25], P De Simone[23], D Decamp[57], M Deckenhoff[10], H Degaudenzi[11,32], L Del Buono[34], C Deplano[42], D Derkach[48], O Deschamps[9], F Dettori[43,44], A Di Canto[4], J Dickens[31], H Dijkstra[11], P Diniz Batista[33], M Dogaru[45], F Domingo Bonal[2,3], S Donleavy[8], F Dordei[4], A Dosil Suárez[5], D Dossett[27], A Dovbnya[58], F Dupertuis[32], R Dzhelyadin[24], A Dziurda[56], A Dzyuba[13], S Easo[11,59], U Egede[39], V Egorychev[29,15], S Eidelman[40,41], D van Eijk[1], S Eisenhardt[35], U Eitschberger[10], R Ekelhof[10], L Eklund[12], I El Rifai[9],

C Elsasser[19], D Elsby[60], A Falabella[48,61], C Färber[4], G Fardell[35], C Farinelli[1], S Farry[37], V Fave[32], D Ferguson[35], V Fernandez Albor[5], F Ferreira Rodrigues[33], M Ferro-Luzzi[11], S Filippov[62], C Fitzpatrick[11], M Fontana[22], F Fontanelli[52,53], R Forty[11], O Francisco[15], M Frank[11], C Frei[11], M Frosini[17,18], S Furcas[46], E Furfaro[50], A Gallas Torreira[5], D Galli[48,49], M Gandelman[15], P Gandini[54], Y Gao[55], J Garofoli[25], P Garosi[21], J Garra Tico[31], L Garrido[2], C Gaspar[11], R Gauld[54], E Gersabeck[4], M Gersabeck[21], T Gershon[11,27], P Ghez[57], V Gibson[31], V V Gligorov[11], C Göbel[28], D Golubkov[29,15], A Golutvin[11,15,29,39], A Gomes[15], H Gordon[54], M Grabalosa Gándara[9], R Graciani Diaz[2], L A Granado Cardoso[11], E Graugés[2], G Graziani[17], A Grecu[45], E Greening[54], S Gregson[31], O Grünberg[4,63], B Gui[25], E Gushchin[62], Yu Guz[24], T Gys[11], C Hadjivasiliou[25], G Haefeli[32], C Haen[11], S C Haines[31], S Hall[39], T Hampson[6], S Hansmann-Menzemer[4], N Harnew[54], S T Harnew[6], J Harrison[21], P F Harrison[27], T Hartmann[4,63], J He[16], V Heijne[1], K Hennessy[8], P Henrard[9], J A Hernando Morata[5], E van Herwijnen[11], E Hicks[8], D Hill[54], M Hoballah[9], C Hombach[21], P Hopchev[57], W Hulsbergen[1], P Hunt[54], T Huse[8], N Hussain[54], D Hutchcroft[8], D Hynds[12], V Iakovenko[64], P Ilten[37], R Jacobsson[11], A Jaeger[4], E Jans[1], F Jansen[1], P Jaton[32], F Jing[55], M John[54], D Johnson[54], C R Jones[31], B Jost[11], M Kaballo[10], S Kandybei[58], M Karacson[11], T M Karbach[11], I R Kenyon[60], U Kerzel[11], T Ketel[43,44], A Keune[32], B Khanji[46], O Kochebina[16], I Komarov[32,36], R F Koopman[43,44], P Koppenburg[1], M Korolev[36], A Kozlinskiy[1], L Kravchuk[62], K Kreplin[4], M Kreps[27], G Krocker[4], P Krokovny[40,41], F Kruse[10], M Kucharczyk[46,47,56], V Kudryavtsev[40,41], T Kvaratskheliya[11,15,29], V N La Thi[32], D Lacarrere[11], G Lafferty[21], A Lai[42], D Lambert[35], R W Lambert[43,44], E Lanciotti[11], G Lanfranchi[11,23], C Langenbruch[11], T Latham[27], C Lazzeroni[60], R Le Gac[7], J van Leerdam[1], J-P Lees[57], R Lefèvre[9], A Leflat[11,36], J Lefrançois[16], O Leroy[7], Y Li[55], L Li Gioi[9], M Liles[8], R Lindner[11], C Linn[4], B Liu[55], G Liu[11], J von Loeben[46], J H Lopes[15], E Lopez Asamar[2], N Lopez-March[32], H Lu[55], J Luisier[32], H Luo[35], F Machefert[16], I V Machikhiliyan[15,29,57], F Maciuc[45], O Maev[11,13], S Malde[54], G Manca[42,65], G Mancinelli[7], N Mangiafave[31], U Marconi[48], R Märki[32], J Marks[4], G Martellotti[14], A Martens[34], L Martin[54], A Martín Sánchez[16], M Martinelli[1], D Martinez Santos[43,44], D Martins Tostes[15], A Massafferri[33], R Matev[11], Z Mathe[11], C Matteuzzi[46], M Matveev[13], E Maurice[7], A Mazurov[11,30,61,62], J McCarthy[60], R McNulty[37], B Meadows[20,25,54], F Meier[10], M Meissner[4], M Merk[1], D A Milanes[66], M-N Minard[57], J Molina Rodriguez[28], S Monteil[9], D Moran[21], P Morawski[56], R Mountain[25], I Mous[1], F Muheim[35], K Müller[19], R Muresan[45], B Muryn[67], B Muster[32], P Naik[6], T Nakada[32], R Nandakumar[59], I Nasteva[33], M Needham[35], N Neufeld[11], A D Nguyen[32], T D Nguyen[32], C Nguyen-Mau[32,68], M Nicol[16], V Niess[9], R Niet[10], N Nikitin[36], T Nikodem[4], S Nisar[25,69], A Nomerotski[54], A Novoselov[24], A Oblakowska-Mucha[67], V Obraztsov[24], S Oggero[1], S Ogilvy[12], O Okhrimenko[64], R Oldeman[11,42,65], M Orlandea[45], J M Otalora Goicochea[15], P Owen[39], B K Pal[25], A Palano[66,70],

M Palutan[23], J Panman[11], A Papanestis[59], M Pappagallo[12], C Parkes[21], C J Parkinson[39], G Passaleva[17], G D Patel[8], M Patel[39], G N Patrick[59], C Patrignani[52,53], C Pavel-Nicorescu[45], A Pazos Alvarez[5], A Pellegrino[1], G Penso[14,71], M Pepe Altarelli[11], S Perazzini[48,49], D L Perego[46,47], E Perez Trigo[5], A Pérez-Calero Yzquierdo[2], P Perret[9], M Perrin-Terrin[7], G Pessina[46], K Petridis[39], A Petrolini[52,53], A Phan[25], E Picatoste Olloqui[2], B Pietrzyk[57], T Pilař[27], D Pinci[14], S Playfer[35], M Plo Casasus[5], F Polci[34], G Polok[56], A Poluektov[27,40,41], E Polycarpo[15], D Popov[22], B Popovici[45], C Potterat[2], A Powell[54], J Prisciandaro[32], V Pugatch[64], A Puig Navarro[32], W Qian[57], J H Rademacker[6], B Rakotomiaramanana[32], M S Rangel[15], I Raniuk[58], N Rauschmayr[11], G Raven[43,44], S Redford[54], M M Reid[27], A C dos Reis[33], S Ricciardi[59], A Richards[39], K Rinnert[8], V Rives Molina[2], D A Roa Romero[9], P Robbe[16], E Rodrigues[21], P Rodriguez Perez[5], G J Rogers[31], S Roiser[11], V Romanovsky[24], A Romero Vidal[5], J Rouvinet[32], T Ruf[11], H Ruiz[2], G Sabatino[14,51], J J Saborido Silva[5], N Sagidova[13], P Sail[12], B Saitta[42,65], C Salzmann[19], B Sanmartin Sedes[5], M Sannino[52,53], R Santacesaria[14], C Santamarina Rios[5], E Santovetti[50,51], M Sapunov[7], A Sarti[23,71], C Satriano[14,26], A Satta[50], M Savrie[30,61], D Savrina[15,29,36], P Schaack[39], M Schiller[43,44], H Schindler[11], S Schleich[10], M Schlupp[10], M Schmelling[22], B Schmidt[11], O Schneider[32], A Schopper[11], M-H Schune[16], R Schwemmer[11], B Sciascia[23], A Sciubba[23,71], M Seco[5], A Semennikov[15,29], K Senderowska[67], I Sepp[39], N Serra[19], J Serrano[7], P Seyfert[4], M Shapkin[24], I Shapoval[11,58], P Shatalov[15,29], Y Shcheglov[13], T Shears[8,11], L Shekhtman[40,41], O Shevchenko[58], V Shevchenko[15,29], A Shires[39], R Silva Coutinho[27], T Skwarnicki[25], N A Smith[8], E Smith[54,59], M Smith[21], K Sobczak[9], M D Sokoloff[20,25], F J P Soler[12], F Soomro[11,23], D Souza[6], B Souza De Paula[15], B Spaan[10], A Sparkes[35], P Spradlin[12], F Stagni[11], S Stahl[4], O Steinkamp[19], S Stoica[45], S Stone[25], B Storaci[19], M Straticiuc[45], U Straumann[19], V K Subbiah[11], S Swientek[10], V Syropoulos[43,44], M Szczekowski[72], P Szczypka[11,32], T Szumlak[67], S T'Jampens[57], M Teklishyn[16], E Teodorescu[45], F Teubert[11], C Thomas[54], E Thomas[11], J van Tilburg[4], V Tisserand[57], M Tobin[19], S Tolk[43,44], D Tonelli[11], S Topp-Joergensen[54], N Torr[54], E Tournefier[39,57], S Tourneur[32], M T Tran[32], M Tresch[19], A Tsaregorodtsev[7], P Tsopelas[1], N Tuning[1], M Ubeda Garcia[11], A Ukleja[72], D Urner[21], U Uwer[4], V Vagnoni[48], G Valenti[48], R Vazquez Gomez[2], P Vazquez Regueiro[5], S Vecchi[30], J J Velthuis[6], M Veltri[17,73], G Veneziano[32], M Vesterinen[11], B Viaud[16], D Vieira[15], X Vilasis-Cardona[2,3], A Vollhardt[19], D Volyanskyy[22], D Voong[6], A Vorobyev[13], V Vorobyev[40,41], C Voß[4,63], H Voss[22], R Waldi[4,63], R Wallace[37], S Wandernoth[4], J Wang[25], D R Ward[31], N K Watson[60], A D Webber[21], D Websdale[39], M Whitehead[27], J Wicht[11], J Wiechczynski[56], D Wiedner[4], L Wiggers[1], G Wilkinson[54], M P Williams[27,59], M Williams[39,74], F F Wilson[59], J Wishahi[10], M Witek[56], S A Wotton[31], S Wright[31], S Wu[55], K Wyllie[11], Y Xie[11,35], F Xing[54], Z Xing[25], Z Yang[55], R Young[35], X Yuan[55], O Yushchenko[24], M Zangoli[48], M Zavertyaev[22,75], F Zhang[55], L Zhang[25], W C Zhang[37], Y Zhang[55], A Zhelezov[4], A Zhokhov[15,29], L Zhong[55] and A Zvyagin[11]

[1] Nikhef National Institute for Subatomic Physics, Amsterdam, The Netherlands
[2] Universitat de Barcelona, Barcelona, Spain
[3] LIFAELS, La Salle, Universitat Ramon Llull, Barcelona, Spain
[4] Physikalisches Institut, Ruprecht-Karls-Universität Heidelberg, Heidelberg, Germany
[5] Universidad de Santiago de Compostela, Santiago de Compostela, Spain
[6] H H Wills Physics Laboratory, University of Bristol, Bristol, UK
[7] CPPM, Aix-Marseille Université, CNRS/IN2P3, Marseille, France
[8] Oliver Lodge Laboratory, University of Liverpool, Liverpool, UK
[9] Clermont Université, Université Blaise Pascal, CNRS/IN2P3, LPC, Clermont-Ferrand, France
[10] Fakultät Physik, Technische Universität Dortmund, Dortmund, Germany
[11] European Organization for Nuclear Research (CERN), Geneva, Switzerland
[12] School of Physics and Astronomy, University of Glasgow, Glasgow, UK
[13] Petersburg Nuclear Physics Institute (PNPI), Gatchina, Russia
[14] Sezione INFN di Roma La Sapienza, Roma, Italy
[15] Universidade Federal do Rio de Janeiro (UFRJ), Rio de Janeiro, Brazil
[16] LAL, Université Paris-Sud, CNRS/IN2P3, Orsay, France
[17] Sezione INFN di Firenze, Firenze, Italy
[18] Università di Firenze, Firenze, Italy
[19] Physik-Institut, Universität Zürich, Zürich, Switzerland
[20] University of Cincinnati, Cincinnati, OH, USA
[21] School of Physics and Astronomy, University of Manchester, Manchester, UK
[22] Max-Planck-Institut für Kernphysik (MPIK), Heidelberg, Germany
[23] Laboratori Nazionali dell'INFN di Frascati, Frascati, Italy
[24] Institute for High Energy Physics (IHEP), Protvino, Russia
[25] Syracuse University, Syracuse, NY, USA
[26] Università della Basilicata, Potenza, Italy
[27] Department of Physics, University of Warwick, Coventry, UK
[28] Pontifícia Universidade Católica do Rio de Janeiro (PUC-Rio), Rio de Janeiro, Brazil
[29] Institute of Theoretical and Experimental Physics (ITEP), Moscow, Russia
[30] Sezione INFN di Ferrara, Ferrara, Italy
[31] Cavendish Laboratory, University of Cambridge, Cambridge, UK
[32] Ecole Polytechnique Fédérale de Lausanne (EPFL), Lausanne, Switzerland
[33] Centro Brasileiro de Pesquisas Físicas (CBPF), Rio de Janeiro, Brazil
[34] LPNHE, Université Pierre et Marie Curie, Université Paris Diderot, CNRS/IN2P3, Paris, France
[35] School of Physics and Astronomy, University of Edinburgh, Edinburgh, UK
[36] Institute of Nuclear Physics, Moscow State University (SINP MSU), Moscow, Russia
[37] School of Physics, University College Dublin, Dublin, Ireland
[38] Università di Modena e Reggio Emilia, Modena, Italy
[39] Imperial College London, London, UK
[40] Budker Institute of Nuclear Physics (SB RAS), Novosibirsk, Russia
[41] Novosibirsk State University, Novosibirsk, Russia
[42] Sezione INFN di Cagliari, Cagliari, Italy
[43] Nikhef National Institute for Subatomic Physics, Amsterdam, The Netherlands
[44] VU University Amsterdam, Amsterdam, The Netherlands
[45] Horia Hulubei National Institute of Physics and Nuclear Engineering, Bucharest-Magurele, Romania
[46] Sezione INFN di Milano Bicocca, Milano, Italy
[47] Università di Milano Bicocca, Milano, Italy
[48] Sezione INFN di Bologna, Bologna, Italy
[49] Università di Bologna, Bologna, Italy
[50] Sezione INFN di Roma Tor Vergata, Roma, Italy
[51] Università di Roma Tor Vergata, Roma, Italy
[52] Sezione INFN di Genova, Genova, Italy
[53] Università di Genova, Genova, Italy
[54] Department of Physics, University of Oxford, Oxford, UK
[55] Center for High Energy Physics, Tsinghua University, Beijing, People's Republic of China
[56] Henryk Niewodniczanski Institute of Nuclear Physics of the Polish Academy of Sciences, Kraków, Poland
[57] LAPP, Université de Savoie, CNRS/IN2P3, Annecy-Le-Vieux, France
[58] NSC Kharkiv Institute of Physics and Technology (NSC KIPT), Kharkiv, Ukraine

[59] STFC Rutherford Appleton Laboratory, Didcot, UK
[60] University of Birmingham, Birmingham, UK
[61] Università di Ferrara, Ferrara, Italy
[62] Institute for Nuclear Research of the Russian Academy of Sciences (INR RAN), Moscow, Russia
[63] Institut für Physik, Universität Rostock, Rostock, Germany
[64] Institute for Nuclear Research of the National Academy of Sciences (KINR), Kyiv, Ukraine
[65] Università di Cagliari, Cagliari, Italy
[66] Sezione INFN di Bari, Bari, Italy
[67] AGH University of Science and Technology, Kraków, Poland
[68] Hanoi University of Science, Hanoi, Vietnam
[69] Institute of Information Technology, COMSATS, Lahore, Pakistan
[70] Università di Bari, Bari, Italy
[71] Università di Roma La Sapienza, Roma, Italy
[72] National Center for Nuclear Research (NCBJ), Warsaw, Poland
[73] Università di Urbino, Urbino, Italy
[74] Massachusetts Institute of Technology, Cambridge, MA, USA
[75] P N Lebedev Physical Institute, Russian Academy of Science (LPI RAS), Moscow, Russia

E-mail: ronan.mcnulty@ucd.ie

Received 29 January 2013
Published 28 February 2013
Online at stacks.iop.org/JPhysG/40/045001

Abstract

Exclusive J/ψ and $\psi(2S)$ vector meson production has been observed in the dimuon channel using the LHCb detector. The cross-section times branching fractions to two muons with pseudorapidities between 2.0 and 4.5 are measured to be

$$\sigma_{pp\to J/\psi(\to\mu^+\mu^-)}(2.0 < \eta_{\mu^\pm} < 4.5) = 307 \pm 21 \pm 36 \text{ pb},$$
$$\sigma_{pp\to\psi(2S)(\to\mu^+\mu^-)}(2.0 < \eta_{\mu^\pm} < 4.5) = 7.8 \pm 1.3 \pm 1.0 \text{ pb},$$

where the first uncertainties are statistical and the second are systematic. The measurements are found to be in good agreement with results from previous experiments and theoretical predictions. The J/ψ photoproduction cross-section has been measured as a function of the photon-proton centre-of-mass energy. The results are consistent with measurements obtained at HERA and confirm a similar power law behaviour for the photoproduction cross-section.

(Some figures may appear in colour only in the online journal)

1. Introduction

Exclusive vector meson production through photoproduction, $\gamma p \to V p$, has attracted much interest both experimentally and theoretically as it provides a rich testing ground for QCD. At sufficiently high meson masses, perturbative QCD (pQCD) can be used to predict the production cross-section [1–3], but as the masses decrease this approach ceases to work due to non-perturbative effects. Light vector meson production is best described by Regge theory [4], which models the process using soft pomeron exchange. This theory predicts a cross-section which is almost flat with respect to W, the photon–proton centre-of-mass energy. In contrast, the cross-section for exclusive J/ψ production has been observed to have a strong power law

dependence on W [5, 6]. This feature is described in pQCD by a hard pomeron (or two gluon exchange) and the fact that the gluon density in the proton increases rapidly with decreasing x, the fractional momentum of the proton carried by the parton [1]. A consistent description of the transition regime between perturbative and non-perturbative QCD is a challenge.

The cross-section for exclusive J/ψ and $\psi(2S)$ production is calculable within pQCD though with large uncertainties. The simplest leading-order calculation is proportional to $[\alpha_S(m_V^2/4)xg(x, m_V^2/4)]^2$, where m_V is the vector meson mass, $\alpha_S(m_V^2/4)$ is the strong coupling constant and $g(x, m_V^2/4)$ is the gluon parton density function (PDF) evaluated at the relevant scale, $m_V^2/4$. Hence a measurement of these processes at the LHC can constrain the gluon PDF [1].

More exotic effects can also be searched for in this process. The forward acceptance of the LHCb detector is sensitive to W values between 10 and 2000 GeV and allows the gluon density to be probed down to $x = 5 \times 10^{-6}$ [7], lower than any previous experiment at a scale of a few GeV. At a sufficiently low value of x, the strong growth of the gluon density with decreasing x is expected to be restrained by gluon recombination [8]. This saturation effect could be visible as a reduction in the photoproduction cross-section with respect to the power law behaviour at W values accessible at the LHC [9]. Exclusive vector meson production also provides a promising channel to investigate the existence of the odderon [10].

The HERA experiments measured J/ψ photoproduction using electron–proton collisions in the range $20 \leqslant W \leqslant 305$ GeV [5, 6]. The data are consistent with a power law dependence of the form $\sigma = a(W/1\,\text{GeV})^{\delta}$ with $a = 3$ nb and $\delta = 0.72$ [9]. The CDF experiment measured exclusive J/ψ production in proton–antiproton collisions in a similar kinematic range as HERA and found consistent results [11].

This paper presents measurements of the cross-section times branching fractions for exclusive J/ψ and $\psi(2S)$ mesons to produce two muons in the pseudorapidity range $2.0 < \eta_{\mu^\pm} < 4.5$ at a proton–proton centre-of-mass energy of $\sqrt{s} = 7$ TeV. The results are compared with previous experiments and a number of theoretical models. The SuperChic [12] and Starlight [13] models use a parameterization of the HERA results to predict the photoproduction cross-section at the LHC. Motyka and Watt [9] use an equivalent photon approximation combined with a dipole model, which is found to reproduce the main features of the HERA data. Gonçalves and Machado [14] use a colour dipole approach and the colour glass condensate formalism which also agrees with the HERA data. Schäfer and Szczurek [15] use an explicit dynamical model of the photoproduction amplitude, which is evaluated in terms of an unintegrated gluon distribution. This model predicts a cross-section which is higher than that observed at HERA.

2. Detector and data samples

The LHCb detector [16] is a single-arm forward spectrometer covering the pseudorapidity range $2 < \eta < 5$ (forward region), designed for the study of particles containing b or c quarks. The detector includes a high precision tracking system consisting of a silicon-strip vertex detector (VELO) surrounding the proton–proton interaction region, a large-area silicon-strip detector located upstream of a dipole magnet with a bending power of about 4 Tm, and three stations of silicon-strip detectors and straw drift-tubes placed downstream. The combined tracking system has a momentum resolution $\Delta p/p$ that varies from 0.4% at 5 GeV/c to 0.6% at 100 GeV/c, and an impact parameter resolution of 20 μm for tracks with high transverse momentum. Charged hadrons are identified using two ring-imaging Cherenkov detectors. Photon, electron and hadron candidates are identified by a calorimeter system consisting of scintillating-pad (SPD) and pre-shower detectors, an electromagnetic calorimeter and a

hadronic calorimeter. The SPD also provides a measurement of the charged particle multiplicity in an event. Muons are identified by a muon system composed of alternating layers of iron and multiwire proportional chambers. The trigger consists of a hardware stage, based on information from the calorimeter and muon systems, followed by a software stage which applies a full event reconstruction. The VELO also has sensitivity to charged particles with momenta above $\sim$100 MeV/c in the pseudorapidity range $-3.5 < \eta < -1.5$ (backward region) and extends the sensitivity of the forward region to $1.5 < \eta < 5$.

The J/ψ and $\psi(2S)$ mesons are identified through their decay to two muons. The protons are only marginally deflected and remain undetected inside the beam pipe. Therefore the signature for exclusive vector meson production is an event containing two muons and no other activity. The analysis is performed using 36 pb^{-1} of proton–proton collision data collected at LHCb in 2010. In this data taking period, the average number of interactions per bunch crossing varied up to a maximum of about 2.5, with most luminosity accumulated at larger values. In order to identify exclusive candidates, the analysis is restricted to events with a single interaction.

Dedicated Monte Carlo generators have been used to produce signal and background events which are passed through a GEANT4 [17] based detector simulation, the trigger emulation and the event reconstruction chain of the LHCb experiment. Two generators have been used to produce samples of exclusive J/ψ and $\psi(2S)$: STARLIGHT [13] and SUPERCHIC [12]. A sample of χ_c production by double pomeron fusion, which forms a background for the J/ψ analysis, has been produced with SUPERCHIC.

3. Event selection

The hardware trigger used in this analysis requires a single muon track with transverse momentum $p_{\mathrm{T}} > 400$ MeV/c, or two muon tracks both with $p_{\mathrm{T}} > 80$ MeV/c, in coincidence with a low SPD multiplicity (<20 hits). The software trigger used requires either a dimuon with invariant mass greater than 2.9 GeV/c^2, or a dimuon with invariant mass greater than 1 GeV/c^2 with a distance of closest approach of the two muons to each other less than 150 μm and a dimuon p_{T} less than 900 MeV/c.

The selection of exclusive events begins with the requirement of two reconstructed muons in the forward region. It is also required that there are no other tracks and no photons in the detector. Thus rapidity gaps, regions devoid of reconstructed charged and neutral objects, are defined. Requiring just two tracks, produced from a single particle decay, ensures two rapidity gaps which sum to 3.5 units in the forward region. An additional rapidity gap is obtained by requiring that there are no tracks in the backward region. The VELO is able to exclude tracks within a certain rapidity gap depending on the z position from which the tracks originate and the event topology. The mean backward rapidity gap where tracks are excluded is 1.7 with a root mean square of about 0.5. Figure 1 shows that requiring a backward rapidity gap affects the distribution of tracks in the forward region; with a backward rapidity gap required, there is a clear peak at precisely two forward tracks. These are candidates for exclusive production.

Both muons are required to be in the pseudorapidity range $2.0 < \eta_{\mu^\pm} < 4.5$. Muon pair candidates, having invariant masses within 65 MeV/c^2 of the known J/ψ and $\psi(2S)$ mass values [18], are selected.

3.1. Non-resonant background determination

A number of background processes have been considered including a non-resonant contribution, inclusive prompt charmonium production, inelastic photoproduction and

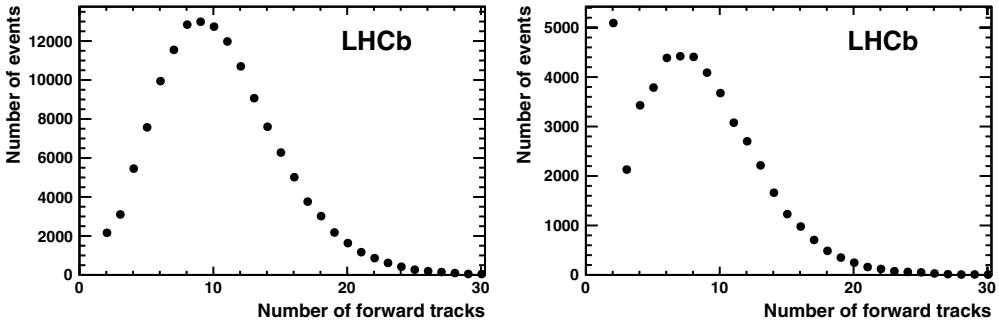

Figure 1. Number of tracks in the forward region for dimuon triggered events which in the backward region have (left) one or more tracks or (right) no tracks.

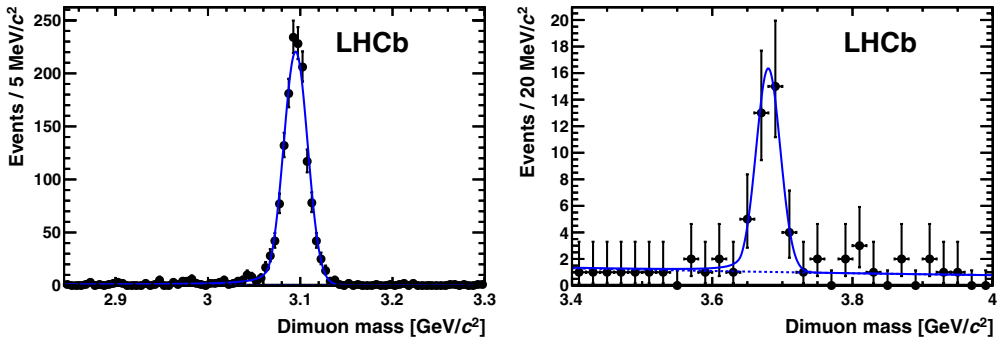

Figure 2. Invariant mass distributions in the regions of (left) the J/ψ and (right) $\psi(2S)$ mass peaks for events with exactly two tracks, no photons and a dimuon with p_{T} below 900 MeV/c. The overall fits to the data are shown by the full curves while the dashed curves show the background contributions.

exclusive χ_c and $\psi(2S) \to J/\psi + X$ productions. The non-resonant background is evaluated by fitting the dimuon invariant-mass distribution, parameterizing the resonances with a crystal ball function [19] and the continuum with an exponential function. Figure 2 displays the fit results. The non-resonant background is estimated to account for $(0.8 \pm 0.1)\%$ and $(16 \pm 3)\%$ of the events within 65 MeV/c^2 of the known J/ψ and $\psi(2S)$ mass values, respectively.

3.2. Inelastic background determination

The requirement of two tracks and no other visible activity enriches the sample in exclusive events. However, this does not guarantee that there is no other activity in the regions outside the LHCb acceptance. The contributions from two non-exclusive processes have been considered: inclusive prompt charmonium produced through colour strings, which leads to large numbers of additional particles; and inelastic J/ψ photoproduction (as shown in figure 3), where gluon radiation or proton dissociation lead to a small number of additional particles. The former has been evaluated using simulated samples of prompt charmonium, generated using PYTHIA [20] and normalized using a data sample where the zero backward tracks requirement has been removed; it is found to be negligible.

The inelastic photoproduction of J/ψ mesons is the dominant background in this analysis. Most of the additional particles produced in these events escape down the beam pipe and thus the inelastic production cross-section as a function of track multiplicity is expected to peak

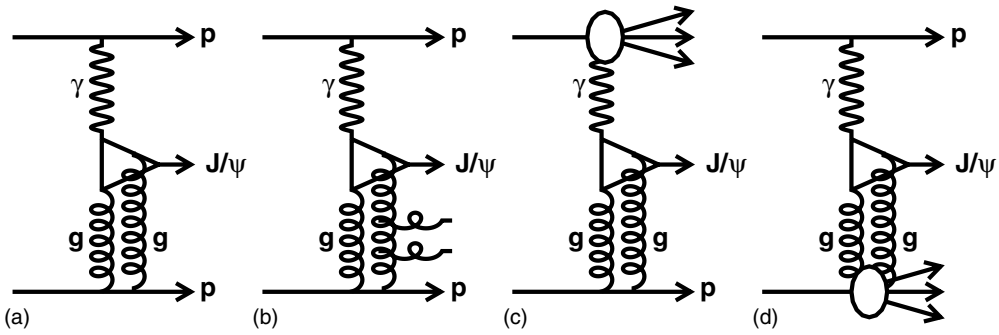

Figure 3. Feynman diagrams displaying (a) exclusive J/ψ photoproduction and (b) inelastic J/ψ photoproduction where a small number of additional particles are produced due to gluon radiation and (c,d) proton dissociation.

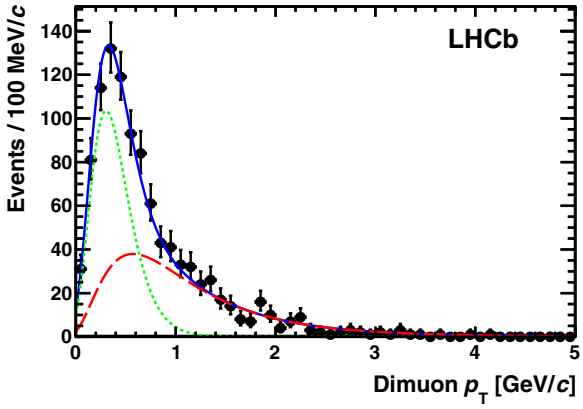

Figure 4. Transverse momentum distribution for exclusive J/ψ candidates with exactly two tracks and no photons. The points represent the data. The fit contains an exclusive signal component (short-dashed green curve) as estimated by SuperChic and an inelastic background component (long-dashed red curve) as estimated from data.

at two tracks. An extrapolation of the inelastic production cross-section from higher track multiplicities is not possible as no reliable simulation is available. Instead, this background is determined from a fit to the p_T spectrum of the exclusive candidates. The signal shape is taken from simulation while the background distribution is estimated from data as described below. The result is shown in figure 4 for events selected by the software trigger, which has no restriction on the dimuon p_T. The agreement between the predictions and the data is good. To reduce the inelastic background contribution the dimuon p_T is required to be less than 900 MeV/c. Below this value the fit estimates that $(70 \pm 4)\%$ of the events are exclusive.

The signal shape is taken from the dimuon p_T distribution of the SuperChic simulation which assumes a ${p_T}^2$ distribution of the form $\exp(-b{p_T}^2)$. Regge theory predicts [4] that the slope, b, of the ${p_T}^2$ distribution increases with W according to

$$b = b_0 + 4\alpha' \ln \frac{W}{W_0}, \tag{1}$$

where fits to H1 and ZEUS data [5, 6] give values of $b_0 = 5\ \mathrm{GeV}^{-2}c^2$, $\alpha' = 0.2\ \mathrm{GeV}^{-2}c^2$ at a scale $W_0 = 90$ GeV. Producing an object of mass m_V at a rapidity y accesses W values of

$$(W_\pm)^2 = m_V \sqrt{s} \exp(\pm|y|), \tag{2}$$

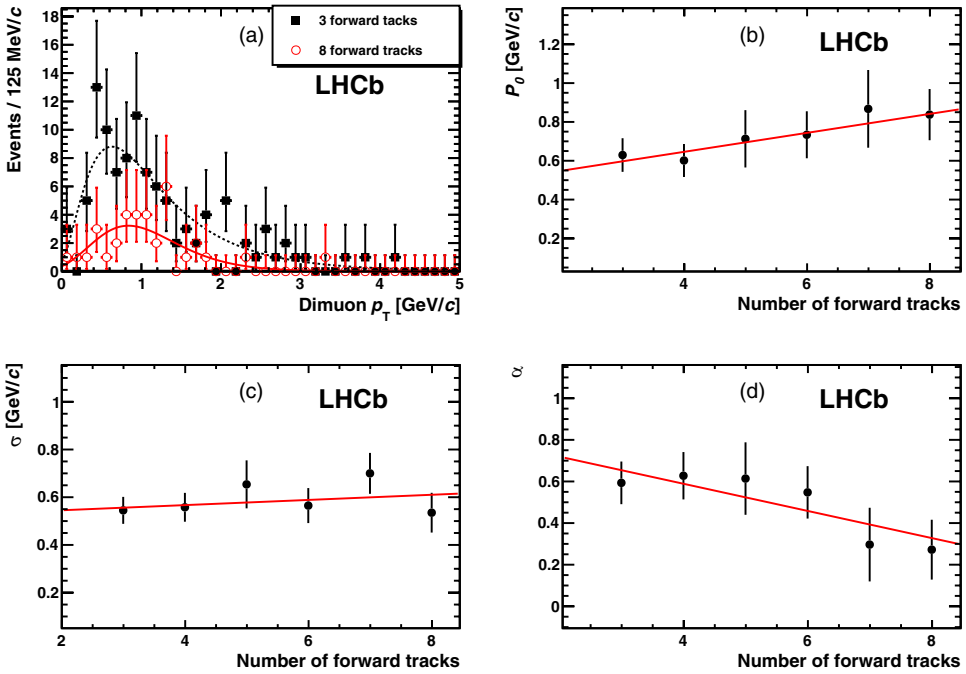

Figure 5. (a) Transverse momentum distribution in J/ψ events with no backward tracks and no photons when there are three (black squares) and eight (red open circles) forward tracks. The results of fitting a Novosibirsk function to the three and eight forward track data are represented by the dashed black and the full red curves respectively. The values for (b) P_0, (c) σ and (d) α of the J/ψ p_T distribution are shown as a function of the number of forward tracks.

where the two solutions, W_+ and W_-, correspond to the photon being either an emitter or a target. The total cross-section has contributions coming from both W_+ and W_-, the relative amounts of which can be determined from the photon energy spectrum of the proton given in [21]. To determine an appropriate b value to describe the p_T spectrum in LHCb, the rapidity range $2.0 < y < 4.5$ is split into ten equally sized bins and $W_\pm$ values are calculated for each bin using equation (2). Two corresponding b values are found using equation (1) and then weighted according to the photon energy spectrum. The mean and root mean square of b in the rapidity bins are 6.1 $\text{GeV}^{-2}c^2$ and 0.3 $\text{GeV}^{-2}c^2$, respectively. These values are consistent with the results of the fit described below where b is left as a free parameter.

The shape for the inelastic background is taken from data. Non-exclusive candidates are selected by requiring events to contain more than two tracks in the forward region. The p_T distributions for events with 3, 4, 5, 6, 7 and 8 forward tracks are each fitted separately with a Novosibirsk function[76], which is a skewed Gaussian function with three parameters for the peak position (P_0), width (σ) and tail (α).

Figure 5(a) displays two of the fitted p_T spectra for the J/ψ meson in events with no backward tracks and no photons when there are 3 and 8 forward tracks. The values for P_0, σ and α are extracted from each fit and plotted as a function of the number of forward tracks in figures 5(b)–(d), respectively. A linear extrapolation of each parameter is made to predict the

[76] The Novosibirsk function is defined as

$$N(P; P_0, \sigma, \alpha) = A \exp(-0.5(\ln^2(1 + \Lambda\alpha(P - P_0))/\alpha^2 + \alpha^2))$$

where $\Lambda = \sinh(\alpha\sqrt{\ln 4})/(\sigma\alpha\sqrt{\ln 4})$, P_0 is the peak position, σ is the width and α is the tail parameter.

inelastic background shape for events with two forward tracks giving $P_0 = 0.55 \pm 0.09\,\text{GeV}/c$, $\sigma = 0.56 \pm 0.06\,\text{GeV}/c$ and $\alpha = 0.72 \pm 0.11$.

Although a full theoretical prediction is not possible [22] a dependence of the p_T peak position on the number of tracks is expected from general kinematic considerations; additional gluon radiation will impart a greater p_T to the J/ψ as well as giving extra tracks inside LHCb, while proton disintegration, leading to additional tracks, is also more likely to occur at higher p_T. This is found to be the case for a number of related processes using simulated events: single and central diffractive events in PYTHIA; the diphoton production of muon pairs with similar masses to the J/ψ in which one or both of the protons disintegrate, as described by LPAIR [23]; and minimum bias events in PYTHIA. A linear dependence is also observed in $Z \to \mu^+\mu^-$ events in data although the average p_T is one order of magnitude larger than in exclusive J/ψ production.

Systematic uncertainties on the inelastic background determination due to both the signal and background shapes have been assessed. To determine the former, the fit to the data is repeated leaving b as a free parameter, which returns a value of $5.8 \pm 0.8\,\text{GeV}^{-2}c^2$. A variation in the estimated percentage of exclusive events of 4% is observed when b is changed by $\pm 1\,\text{GeV}^{-2}c^2$. The uncertainty due to the background shape is found by varying the parameters of the phenomenological shape within their statistical uncertainties resulting in a change of 4% in the estimated fraction of exclusive events. Therefore, it is estimated that $(70 \pm 4 \pm 6)\%$ of the J/ψ sample consists of exclusive events, where the first uncertainty is statistical and the second is systematic due to out understanding of the signal and background shapes. It is assumed that the $\psi(2S)$ sample has the same proportion of exclusive events.

3.3. Exclusive feed-down background determination

Exclusive χ_c production can feed down to give a fake exclusive J/ψ, via the $\chi_c \to J/\psi\,\gamma$ decay, when the photon is very soft or is outside the detector acceptance. There is no corresponding resonance above the $\psi(2S)$. Exclusive χ_c candidate events are identified in the data as those containing a J/ψ and a single photon. The background from χ_c feed-down is then estimated by scaling the number of observed χ_c candidates by the ratio of fake exclusive J/ψ to exclusive χ_c candidates in simulated χ_c events. The feed-down from χ_c decay is estimated to account for $(9.0 \pm 0.8)\%$ of the exclusive J/ψ candidates, where the uncertainty includes a contribution due to the uncertainty on the photon reconstruction efficiency in simulation.

Exclusive $\psi(2S)$, in particular $\psi(2S) \to J/\psi + X$, can also feed down to give a fake exclusive J/ψ if the additional particles are undetected. This is estimated from a simulated sample of $\psi(2S)$ events which has been normalized using the number of observed $\psi(2S) \to \mu^+\mu^-$ events in data. The amount of feed-down to the J/ψ from the $\psi(2S)$ is estimated to be $(1.8 \pm 0.3)\%$.

3.4. Selection summary

The requirements for the selection of exclusive J/ψ and $\psi(2S)$ events are summarized in table 1. In total, 1492 exclusive J/ψ and 40 exclusive $\psi(2S)$ candidate events pass the selection requirements. The overall purities (including inelastic, non-resonant, and feed-down backgrounds where appropriate) are estimated to be $(62 \pm 4 \pm 5)\%$ for the J/ψ sample and $(59 \pm 4 \pm 5)\%$ for the $\psi(2S)$ sample.

A cross-section times branching fraction, $\sigma_{V\to\mu^+\mu^-}$, is calculated for the J/ψ and the $\psi(2S)$ using the number of selected events, N, and the equation $\sigma_{V\to\mu^+\mu^-} = pN/(\epsilon L)$ where

Table 1. Summary of selection requirements.

Quantity	Requirement
Dimuon mass	within 65 MeV/c^2 of known value
Dimuon p_{T}	$p_{\mathrm{T}} < 900$ MeV/c
Muon η	$2.0 < \eta_{\mu^\pm} < 4.5$
Number of backward tracks	0
Number of forward tracks	2
Number of photons	0

ϵ represents the efficiency for selecting the events, p is the purity of the sample, and L is the luminosity which has been determined with an uncertainty of 3.5% [24].

4. Efficiency determination

The efficiency ϵ is the product of five components, $\epsilon_{\mathrm{trigger}} \times \epsilon^2_{\mathrm{track}} \times \epsilon^2_{\mathrm{muon}} \times \epsilon_{\mathrm{sel}} \times \epsilon_{\mathrm{single}}$ where: $\epsilon_{\mathrm{trigger}}$ is the efficiency for triggering on events that pass the offline selection; $\epsilon_{\mathrm{track}}$ is the efficiency for reconstructing a track within the fiducial region of the measurement; ϵ_{muon} is the efficiency for identifying a track as a muon; ϵ_{sel} is the efficiency of the selection requirements in the kinematic range of the measurement; and $\epsilon_{\mathrm{single}}$ is the efficiency for selecting single interaction events. The first four components have been determined from simulation. The fifth component accounts for the fact that the selection requirements reject signal events that are accompanied by a visible proton–proton interaction in the same beam crossing.

The number of visible proton–proton interactions per beam crossing, n, is assumed to follow a Poisson distribution, $P(n) = \mu^n \exp(-\mu)/n!$, where μ is the average number of visible interactions. The probability that a signal event is not rejected due to the presence of another visible interaction is given by $P(0)$ and, therefore, $\epsilon_{\mathrm{single}} = \exp(-\mu)$. This has been calculated throughout the data-taking period in roughly hour-long intervals. Variations in μ during this interval have been studied and found to have a negligible effect. The spread in the value of μ for different crossing bunch-pairs is small and its effect is neglected. The impact of detector noise has also been investigated using data taken when either one beam or no beam circulated and a systematic uncertainty of 0.7% is evaluated leading to a determination for $\epsilon_{\mathrm{single}}$ of $(21.1 \pm 0.1)\%$.

A systematic uncertainty of 4% is assigned to $\epsilon_{\mathrm{trigger}}$. This is based on the difference between the value measured in data and in simulation as determined in [25].

A tag-and-probe technique with $J/\psi \to \mu^+\mu^-$ decays [26] has been used to study $\epsilon_{\mathrm{track}}$. The estimated value from this method is found to agree within 1% with the simulation. This value is taken as a systematic uncertainty per track.

A systematic uncertainty of 2.5% per muon is assigned to the determination of ϵ_{muon}. This is based on the results from [25] using a tag-and-probe technique.

The fraction of exclusive J/ψ mesons below the p_{T} selection threshold of 900 MeV/c is found to vary by 1% when b, the p_{T} shape parameter, is changed by ± 1 GeV$^{-2}c^2$. Thus a systematic uncertainty of 1%, due to the uncertainty in the p_{T} shape, is assigned to the determination of ϵ_{sel}. No systematic uncertainty is assigned due to the J/ψ polarization; it is assumed to be transversely polarized due to s-channel helicity conservation. A summary of the systematic uncertainties of the analysis is shown in table 2.

Table 2. Relative systematic uncertainties on the measurement.

Source	Uncertainty (%)
Luminosity	3.5
Trigger efficiency	4
Tracking efficiency	2
Identification efficiency	5
Selection efficiency	1
Single interaction efficiency	0.7
$\psi(2S)$ background (J/ψ analysis)	0.3
χ_c background (J/ψ analysis)	0.8
Signal shape of dimuon p_{T} fit	6
Background shape of dimuon p_{T} fit	6

Table 3. Comparison of cross-section times branching fraction measurements (pb) with theoretical predictions.

Predictions	$\sigma_{pp\to J/\psi\,(\to\mu^+\mu^-)}$	$\sigma_{pp\to\psi(2S)(\to\mu^+\mu^-)}$
Gonçalves and Machado	275	
STARLIGHT	292	6.1
Motyka and Watt	334	
SUPERCHIC[a]	396	
Schäfer and Szczurek	710	17
LHCb measured value	$307 \pm 21 \pm 36$	$7.8 \pm 1.3 \pm 1.0$

[a] SUPERCHIC simulation does not include a gap survival factor.

5. Results

The cross-section times branching fraction to two muons with pseudorapidities between 2.0 and 4.5 is measured for exclusive J/ψ and $\psi(2S)$ to be

$$\sigma_{pp\to J/\psi\,(\to\mu^+\mu^-)}(2.0 < \eta_{\mu^\pm} < 4.5) = 307 \pm 21 \pm 36\ \text{pb},$$

$$\sigma_{pp\to\psi(2S)(\to\mu^+\mu^-)}(2.0 < \eta_{\mu^\pm} < 4.5) = 7.8 \pm 1.3 \pm 1.0\ \text{pb},$$

where the first uncertainty is statistical and the second is systematic.

These results are compared to a number of predictions for exclusive production in table 3. The predictions for STARLIGHT and SUPERCHIC have been determined using samples of generated events with a full LHCb simulation. The other predictions are obtained by scaling the differential cross-section in rapidity for each model by an acceptance factor corresponding to the fraction of mesons at a given rapidity that have both muons in the fiducial volume, as determined using STARLIGHT. For the models of Motyka and Watt, and Gonçalves and Machado, a rescattering correction of 0.8 has been assumed [15]. The prediction of Schäfer and Szczurek is significantly higher than the data; good agreement is observed with all other predictions.

Combining the vector meson branching fractions to two muons with acceptance factors determined from STARLIGHT gives a ratio of $\psi(2S)$ to J/ψ production of 0.19 ± 0.04. This can be compared to a value of 0.16 according to STARLIGHT and about 0.2 according to Schäfer and Szczurek. CDF measured this ratio to be 0.14 ± 0.05 [11] and at HERA it was measured to be 0.166 ± 0.012 [5, 6] although these were at different values of W.

The differential J/ψ cross-section is also measured in ten bins of J/ψ rapidity. The trigger and selection efficiencies are calculated from the simulation in bins of rapidity. The systematic uncertainties are dominated by the purity and the statistical uncertainty coming from the size

Table 4. Cross-section measurements (nb) as a function of J/ψ rapidity.

Rapidity	2.00–2.25	2.25–2.50	2.50–2.75	2.75–3.00
$\frac{d\sigma}{dy}(J/\psi)$	$3.2 \pm 0.8 \pm 0.9$	$4.5 \pm 0.5 \pm 0.8$	$5.3 \pm 0.4 \pm 0.9$	$4.4 \pm 0.3 \pm 0.7$
Rapidity	3.00–3.25	3.25–3.50	3.50–3.75	3.75–4.00
$\frac{d\sigma}{dy}(J/\psi)$	$5.5 \pm 0.3 \pm 0.8$	$4.8 \pm 0.3 \pm 0.7$	$5.2 \pm 0.3 \pm 0.8$	$4.8 \pm 0.4 \pm 0.8$
Rapidity	4.00–4.25	4.25–4.50		
$\frac{d\sigma}{dy}(J/\psi)$	$4.7 \pm 0.5 \pm 0.9$	$4.1 \pm 0.9 \pm 1.3$		

of the simulation sample. The purity within each bin is assumed to be the same as in the integrated sample. An acceptance factor in each rapidity bin has been calculated using the STARLIGHT simulation. Table 4 summarizes the differential cross-section result.

The present results can be compared to H1 and ZEUS results [5, 6] for the photoproduction of J/ψ. This is possible as the underlying production mechanism is the same: at HERA the photon radiates from an electron, while at the LHC the photon radiates from a proton. The differential cross-section for proton–proton exclusive photoproduction of a vector meson with mass m_V can be obtained by weighting the photon-proton exclusive production cross-section by the photon flux, dn/dk, for a photon of energy k [9, 13]

$$\left.\frac{d\sigma}{dy}\right|_{pp\to pVp} = r(y)\left[k_+\frac{dn}{dk_+}\sigma_{\gamma p\to Vp}(W_+) + k_-\frac{dn}{dk_-}\sigma_{\gamma p\to Vp}(W_-)\right], \tag{3}$$

$$k_\pm \approx (m_V/2)\exp(\pm|y|), \tag{4}$$

where $W_\pm$ is defined as in equation (2) and $r(y)$ is an absorptive correction which depends on y [15].

Assuming the validity of a power law dependence of the form aW^δ to describe $\sigma_{\gamma p\to Vp}$, the proton-proton differential cross-section can be written as

$$\left.\frac{d\sigma}{dy}\right|_{pp\to pVp} = a(2\sqrt{s})^{\delta/2}r(y)\left[\frac{dn}{dk_+}{k_+}^{1+\delta/2} + \frac{dn}{dk_-}{k_-}^{1+\delta/2}\right]. \tag{5}$$

The parameters for the power law dependence of the photoproduction cross-section are found by fitting the differential cross-section data from table 4 with the functional form given in equation (5). The uncertainties between bins are taken to be uncorrelated for all sources except for the purity, which is fully correlated between bins. For the description of $\frac{dn}{dk}$, the photon energy spectrum given in [21] is used. The absorptive corrections have been calculated in [15] for proton–proton collisions and have a value of 0.85 at $y = 0$ and 0.75 at $y = 3$ with a rather flat dependence on y. This analysis assumes a shape $r(y) = 0.85 - 0.1|y|/3$. The fit to the data in table 4 gives values of $a = 0.8^{+1.2}_{-0.5}$ nb and $\delta = 0.92 \pm 0.15$ with a χ^2 of 4.3 for eight degrees of freedom, indicating the results are consistent with the hypothesis of a power law dependence. The values obtained are also consistent with the results from HERA, albeit with much larger uncertainties.

5.1. Evaluation of the photon–proton cross-section

The differential cross-sections for the process $pp \to pJ/\psi\, p$ given in table 4 are transformed into cross-sections for the process $\gamma p \to J/\psi\, p$ using a re-arrangement of equation (3)

$$\sigma_{\gamma p\to Vp}(W_\pm) = \frac{1/r(y)\left.\frac{d\sigma}{dy}\right|_{pp\to pVp} - k_\mp\frac{dn}{dk_\mp}\sigma_{\gamma p\to Vp}(W_\mp)}{k_\pm\frac{dn}{dk_\pm}}. \tag{6}$$

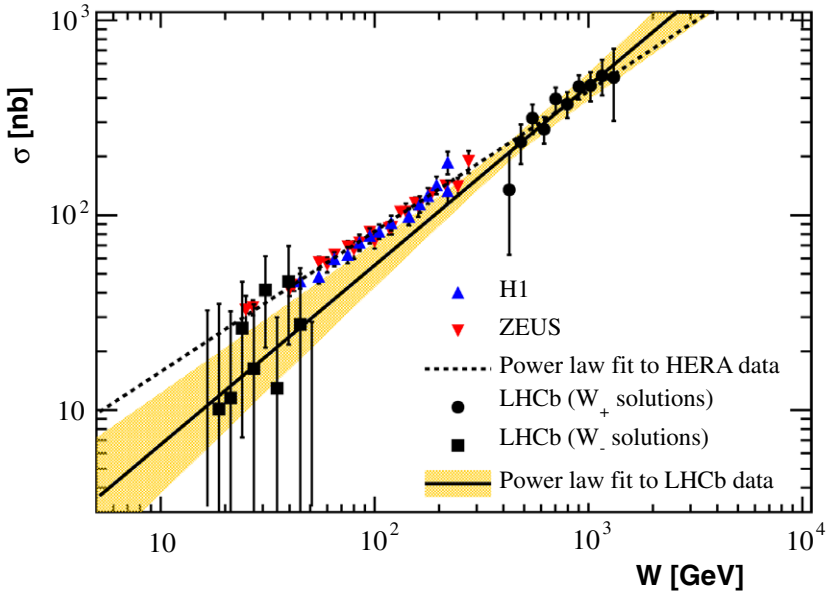

Figure 6. Dependence of J/ψ photoproduction cross-section on the centre-of-mass energy of the photon-proton system. The blue (red) triangles represent the data from H1 (ZEUS) [5, 6]. The black dots and squares are derived from the LHCb differential cross-section as a function of rapidity. The dashed and full lines are the power law dependences determined from the HERA and LHCb data, respectively. The uncertainty on the LHCb power law determination is shown by the shaded band.

The photoproduction cross-sections at W_+ and W_- are determined independently using equation (6) and substituting into the right-hand side the expected cross-section for the alternative W solution from the power law determined above.

The LHCb data are plotted together with the H1 and ZEUS data in figure 6. The power law dependences determined from LHCb data and from HERA data are also indicated. The uncertainty on the LHCb power law determination is shown by the shaded band. Only experimental uncertainties are shown on the LHCb data, which have significant bin-to-bin correlations due to the purity determination. Theoretical uncertainties that account for the power law assumption and the absorptive correction are not included. Both are smaller than the current experimental uncertainties; using the HERA power law in place of the LHCb power law in equation (6) changes the estimated values of $\sigma_{\gamma p\to V p}$ by about half the experimental uncertainty, while changing the absorptive correction by 5% changes $\sigma_{\gamma p\to V p}$ by about one quarter of the experimental uncertainty. With the precision of the current data, the LHCb results are consistent with HERA and confirm a similar power law behaviour for the photoproduction cross-section.

6. Conclusion

The first observations of exclusive J/ψ and $\psi(2S)$ production in proton–proton collisions have been made. The cross-sections times branching fraction to two muons with pseudorapidities between 2.0 and 4.5 are measured to be $307 \pm 21 \pm 36$ pb and $7.8 \pm 1.3 \pm 1.0$ pb for exclusive J/ψ and $\psi(2S)$, respectively.

The measured cross-sections are in agreement with the theoretical predictions of STARLIGHT, SUPERCHIC, Gonçalves and Machado, and Motyka and Watt. The differential cross-section for J/ψ production as a function of rapidity has also been measured. This has allowed the J/ψ photoproduction cross-section as a function of the photon-proton centre-of-mass energy to be determined. The data are consistent with a power law dependence and the parametric form is in broad agreement with previous results from H1 and ZEUS.

Acknowledgments

We thank Lucian Harland-Lang, Valery Khoze, James Stirling and Graeme Watt for many helpful discussions. We express our gratitude to our colleagues in the CERN accelerator departments for the excellent performance of the LHC. We thank the technical and administrative staff at the LHCb institutes. We acknowledge support from CERN and from the national agencies: CAPES, CNPq, FAPERJ and FINEP (Brazil); NSFC (China); CNRS/IN2P3 and Region Auvergne (France); BMBF, DFG, HGF and MPG (Germany); SFI (Ireland); INFN (Italy); FOM and NWO (The Netherlands); SCSR (Poland); ANCS/IFA (Romania); MinES, Rosatom, RFBR and NRC 'Kurchatov Institute' (Russia); MinECo, XuntaGal and GENCAT (Spain); SNSF and SER (Switzerland); NAS Ukraine (Ukraine); STFC (United Kingdom); NSF (USA). We also acknowledge the support received from the ERC under FP7. The Tier1 computing centres are supported by IN2P3 (France), KIT and BMBF (Germany), INFN (Italy), NWO and SURF (The Netherlands), PIC (Spain), GridPP (United Kingdom). We are thankful for the computing resources put at our disposal by Yandex LLC (Russia), as well as to the communities behind the multiple open source software packages that we depend on.

References

[1] Martin A D, Nockles C, Ryskin M and Teubner T 2008 Small x gluon from exclusive J/ψ production *Phys. Lett.* B **662** 252 (arXiv:0709.4406)
[2] Ryskin M G 1993 J/ψ electroproduction in LLA QCD *Z. Phys.* C **57** 89
[3] Ryskin M G, Roberts R G, Martin A D and Levin E M 1997 Diffractive J/ψ photoproduction as a probe of the gluon density *Z. Phys.* C **76** 231 (arXiv:hep-ph/9511228)
[4] Collins P D B 1977 *An Introduction to Regge Theory and High Energy Physics* (Cambridge: Cambridge University Press)
[5] Aktas A *et al* (H1 Collaboration) 2006 Elastic J/ψ production at HERA *Eur. Phys. J.* C **46** 585 (arXiv:hep-ex/0510016)
[6] Chekanov S *et al* (ZEUS Collaboration) 2002 Exclusive photoproduction of J/ψ mesons at HERA *Eur. Phys. J.* C **24** 345 (arXiv:hep-ex/0201043)
[7] Martin A D, Roberts R G, Stirling W J and Thorne R S 2000 Parton distributions and the LHC: W and Z production *Eur. Phys. J.* C **14** 133 (arXiv:hep-ph/9907231)
[8] Golec-Biernat K J and Wusthoff M 1998 Saturation effects in deep inelastic scattering at low q^2 and its implications on diffraction *Phys. Rev.* D **59** 014017 (arXiv:hep-ph/9807513)
[9] Motyka L and Watt G 2008 Exclusive photoproduction at the Fermilab Tevatron and CERN LHC within the dipole picture *Phys. Rev.* D **78** 014023 (arXiv:0805.2113)
[10] Ewerz C 2003 The odderon in quantum chromodynamics arXiv:hep-ph/0306137
[11] Aaltonen T *et al* (CDF Collaboration) 2009 Observation of exclusive charmonium production and $\gamma\gamma \to \mu^+\mu^-$ in $p\bar{p}$ collisions at $\sqrt{s} = 1.96$ TeV *Phys. Rev. Lett.* **102** 242001 (arXiv:0902.1271)
[12] Harland-Lang L A, Khoze V A, Ryskin M G and Stirling W J 2010 Central exclusive χ_c meson production at the Tevatron revisited *Eur. Phys. J.* C **65** 433 (arXiv:0909.4748)
[13] Klein S R and Nystrand J 2004 Photoproduction of quarkonium in proton–proton and nucleus–nucleus collisions *Phys. Rev. Lett.* **92** 142003
[14] Gonçalves V P and Machado M V T 2011 Vector meson production in coherent hadronic interactions: an update on predictions for RHIC and LHC *Phys. Rev.* C **84** 011902 (arXiv:1106.3036)

[15] Schäfer W and Szczurek A 2007 Exclusive photoproduction of J/ψ in proton–proton and proton–antiproton scattering *Phys. Rev.* D **76** 094014 (arXiv:0705.2887)
[16] Alves A A Jr *et al* (LHCb Collaboration) 2008 The LHCb detector at the LHC *J. Instrum.* **3** S08005
[17] Agostinelli S *et al* (GEANT4 Collaboration) 2003 GEANT4: a simulation toolkit *Nucl. Instrum. Methods* A **506** 250
[18] Beringer J *et al* (Particle Data Group) 2012 Review of particle physics *Phys. Rev.* D **86** 010001
[19] Skwarnicki T 1986 A study of the radiative cascade transitions between the Upsilon-prime and Upsilon resonances *PhD Thesis* Institute of Nuclear Physics, Krakow DESY-F31-86-02
[20] Sjöstrand T, Mrenna S and Skands P 2006 PYTHIA 6.4 Physics and manual *J. High Energy Phys.* JHEP05(2006)026 (arXiv:hep-ph/0603175)
[21] Drees M and Zeppenfeld D 1989 Production of supersymmetric particles in elastic ep collisions *Phys. Rev.* D **39** 2536
[22] Harland-Lang L A, Khoze V A, Ryskin M G and Stirling W J 2012 The phenomenology of central exclusive production at hadron colliders *Eur. Phys. J.* C **72** 2110 (arXiv:1204.4803)
[23] Vermaseren J A M 1983 Two-photon processes at very high energies *Nucl. Phys.* B **229** 347
[24] Aaij R *et al* (LHCb Collaboration) 2012 Absolute luminosity measurements with the LHCb detector at the LHC *J. Instrum.* **7** P01010 (arXiv:1110.2866)
[25] Aaij R *et al* (LHCb Collaboration) 2011 Measurement of J/ψ production in pp collisions at $\sqrt{s} = 7$ TeV *Eur. Phys. J.* C **71** 1645 (arXiv:1103.0423)
[26] Jaeger A *et al* 2011 Measurement of the track finding efficiency *CERN-LHCb-PUB-2011-025*